High-Altitude Effects on Three-Dimensional Nonequilibrium Viscous Shock-Layer Flows

D. J. Song* and S. Swaminathan*
Virginia Polytechnic Institute and State University, Blacksburg, Virginia
and
Clark H. Lewis†
VRA, Inc., Blacksburg, Virginia

Three-dimensional finite-rate chemically reacting viscous shock-layer flows over complex geometries have been analyzed using a two-temperature model (electron and heavy particle temperature). For the cases under consideration, the results from the two-temperature model without shock slip agree with those from the one-temperature model. Almost negligible difference in electron concentration across the shock layer was observed between one- and two-temperature models.

Nomenclature

CA	= axial force coefficient
CFSINF	= skin-friction coefficient in the streamwise direction
CI	= denotes C_i
C_i	= concentration of species i, ρ_i/ρ
$E-/CC$	= electron concentration per cm^3
FCW	= fully catalytic wall
FNN	= fully catalytic wall, no shock slip, no wall-slip condition
FSN	= fully catalytic wall, shock slip, no wall-slip condition
H	= stagnation enthalpy, H^*/U_∞^2
NCW	= noncatalytic wall
NEQ	= finite-rate nonequilibrium chemical reactions
NSS	= no shock slip
NWS	= no wall slip
p	= pressure, $p^*/\rho_\infty U_\infty^2$
PG	= perfect gas
PINF	= freestream pressure
PW	= wall pressure
q_w	= heat-transfer rate at the wall
Re	= Reynolds number
Rn^*	= nose radius, m
RN	= denotes Rn^*
SP	= denotes species
SS	= shock slip
STINF	= Stanton number $q_w^*/\rho_\infty U_\infty (H^*_0 - H^*_w)$
s,n,ϕ	= nondimensional surface-normal coordinate system
T	= temperature, T^*/T_{ref}
T_{ref}	= U_∞^2/C_{P_∞}
TE	= electron temperature
U_∞	= freestream velocity, m/s
u,v,w	= streamwise, body normal, and circumferential velocity components
WS	= wall slip
Y	= distance normal to body
ZORN	= z/Rn^*
z,Z	= axial distance
α	= angle of attack, deg
ϵ	= Reynolds number parameter, $\epsilon^2 = \mu_{\text{ref}}/\rho_\infty U_\infty Rn^*$
μ	= viscosity, μ^*/μ_{ref}
ξ,η,ζ	= normalized surface-normal coordinates
ρ	= density, ρ^*/ρ_{ref}

Superscripts

$(\ )^*$	= dimensional variable

Subscripts

i	= species i
ref	= dimensional reference conditions
w	= wall conditions
∞	= dimensional freestream conditions
0	= stagnation conditions

Introduction

AEROASSISTED orbital transfer vehicles (AOTVs) operate at high altitudes in the low-density regime, and the flow is essentially nonequilibrium during most of the flight. The velocities encountered in AOTV applications are relatively high, and reasonably high temperatures are achieved in the shock layer. To take into account the ionization of oxygen and nitrogen atoms and molecules in these temperature ranges, an eleven-species chemical reaction model consisting of O, O_2, N, N_2, NO, NO^+, O^+, O_2^+, N^+, N_2^+, and e^- has been used previously.[1] In that study, the heavy particles and electrons were assigned the same temperature. A recent study of one-dimensional flow behind a normal shock wave[2] has shown that at the freestream conditions in which an AOTV flies, the pressure is sufficient to cause a Maxwellian distribution in translational, rotational, and vibrational modes. However, only the rotational mode on the molecules tends to equilibrate rapidly with the translational mode of the heavy particles (atoms or molecules), and the vibrational temperature of the heavy particles and the translational temperature of electrons are regarded as the same temperature. These assumptions were based on the fact that the energy exchange between the electron translational mode and the vibrational mode of heavy particles is rapid, which is believed to be valid everywhere except in the viscous boundary layer.

However, in this study, following the approach of Leibowitz,[4] due to the large ratio of atom or ion mass-to-electron mass, electrons transfer energy rapidly by collision with other electrons but only slowly by elastic collision with atoms or ions. The number of collisions necessary to produce a Maxwellian velocity distribution between electrons and atoms is

Presented as Paper 84-0304 at the AIAA 22nd Aerospace Sciences Meeting, Reno, Nev., Jan. 9-12, 1984; submitted July 13, 1984; revision received March 6, 1985.

*Graduate Student, Aerospace and Ocean Engineering Department.
†President. Associate Fellow AIAA.

larger than the number of collisions necessary to produce a Maxwellian distribution among electrons by a factor of the mass ratio. Hence, two separate Maxwellian distributions are necessary to describe the population of electrons and heavy particles, and thus the electrons are assigned a different temperature.

Studies[3-5] on the nonequilibrium viscous flow around Jovian entry bodies have shown that there can be a substantial difference between electron and heavy-particle temperatures during the ionization relaxation. In the present study, the viscous shock-layer code using an eleven-species model (VSLNQ11)[1] has been modified to include a two-temperature model. The electron concentration across the shock-layer would be very important to the transmission of electromagnetic signals to and from a re-entry vehicle. The major objective is the accurate prediction of electron concentration during the high-altitude nonequilibrium flight. This knowledge will enhance our ability to calculate the electron concentration in the wake of a re-entry vehicle.

Results from the two-temperature model have been compared to those from the one-temperature model. Although the two codes are capable of analyzing straight and bent multiconics, a sphere cone has been selected as test cases for demonstration purposes.

The geometry considered is a 9-deg half-angle sphere cone with a nose radius of 0.1524 m (6 in.). The length of the body is 20 nose radii. The body was analyzed at altitude conditions of 83.82 km (275,000 ft) and at two freestream velocities, namely, 7620 m/s (25,000 ft/s) and 10,606 m/s (35,000 ft/s). The wall temperatures for both cases were maintained at 1000 K. The details of the test conditions are given in Table 1.

Analysis

The governing equations are derived from the steady Navier-Stokes equation for a reacting gas mixture as given by Bird et al.[6] and are written in a body-oriented orthogonal coordinate system (see Fig. 1). The s coordinate is tangent to the body in the streamwise direction, the n coordinate is normal to the surface, and the ϕ coordinate is the angle around the body measured from the windward streamline. The governing equations are given by Swaminathan.[7] The electron temperature is obtained by solving the electron energy equation. The electron energy equation for a hydrogen-helium system has been given by Leibowitz[4] for a one-dimensional steady shock wave. Leibowitz has used the Appleton-Bray formulation for hydrogen-helium mixture, thereby suggesting a weak heavy-particle vibrational mode and electron temperature coupling for hydrogen between a shock velocity 13-20 km/s in a 0.208 H_2-0.792 He mixture. The helium-hydrogen results show significant difference between heavy-particle temperature and electron temperature during much of the ionization process. The same electron energy equation and procedure are applied to high-temperature air. The details of the derivation of electron energy equations for the oxygen and nitrogen system are presented in Appendix A.

At the test case conditions of the present study, the Knudsen number approaches 0.052. The effects of low-density flow would become significant both at the surface and at the shock. However, the surface slip and temperature jump conditions were not used. The shock boundary conditions with slip are the modified Rankine-Hugoniot equations given by Swaminathan et al.[8]

The wall can be fully catalytic ($C_{O_2} = 0.23456$, $C_{N_2} = 0.76544$), finite catalytic, or noncatalytic ($\partial C_i/\partial \eta = 0$). The details of catalytic wall boundary conditions are given by Kim.[9] The input shock for the viscous shock layer code was obtained from an inviscid flowfield code, NOL3D.[10,11]

The multicomponent gas mixture is considered to be a mixture of thermally perfect gases, and the thermodynamic and transport properties for each species were calculated using the local heavy-particle temperature. The properties for the gas mixture were then determined in terms of the properties of individual species. The enthalpy and specific heat data of the species were obtained from the thermodynamic data of Browne.[12-14] The viscosity of each of the individual species as a function of temperature was obtained from Biolsi,[15] and the data were fitted as quadratics on log-log plots. The thermal conductivity of the individual species was calculated from the Eucken semiempirical formula. Knowing the viscosity and thermal conductivity of the individual species, the viscosity and the thermal conductivities of the mixture were calculated using Wilke's semiempirical relation. In the present work, the diffusion model is limited to binary diffusion with a Lewis number of 1.4.

In the present study, it is assumed that the fluid medium is a mixture of reacting species and that the chemical reactions proceed at a finite rate. The production terms occurring in the energy equation and the species concentration equations are obtained from the various chemical reactions among the individual species. In the present study, the eleven-species model (O, O_2, N, N_2, NO, NO^+, N^+, N_2^+, O^+, O_2^+, and e^-) was used. The reaction-rate data for the eleven-species model were obtained from Kang and Dunn.[16] The modifications necessary for the two-temperature model were incorporated into the eleven-species code. For the solution of the electron energy equation, the cross section of elastic collisions between electrons and the heavy particles are required. The elastic collision cross sections between electron and oxygen are taken from Neynaber et al.,[17] whereas those for nitrogen are taken from Capatelli and Devote.[18] As an initial estimate, the Coulomb cross sections for O^+ and N^+ were assumed to be the same as their respective elastic collision cross sections.

Results and Discussion

The results from the present study are the effects of the two-temperature model on the electron density profile and the surface-measurable quantities for various freestream conditions. As mentioned earlier, the two-temperature model has been incorporated into the eleven-species code (VSLNQ11). The electron density profiles are compared to those from the seven-species code and RAM C flight data. RAM C flights were part of a program conducted by NASA Langley Research Center for studying flowfield electron concentration under re-entry conditions.

Effects of Two-Temperature Model

Figures 2 to 5 show the temperature and electron density profiles for case 1 at $\alpha = 0$ and 5 deg. The wall was assumed to be fully catalytic, and no-slip conditions were assumed at the wall and shock. The electron temperature and heavy-particle

Table 1 Test case freestream conditions

		Freestream conditions							
Geometry	Rn, m	α, deg	Alt, m	U_∞, m/s	ρ_∞, Amagats	T_∞, K	$Re_{,Rn}$	ϵ	Tw, K
Case 1 (RAMC)	0.1526	0&5	83820	7620	7.661E-6	182.16	937.4	0.1745	1000
Case 2		0	83820	10606.1	7.661E-6	182.16	1312.3	0.1746	1000

temperature profiles are nearly identical for the freestream condition considered. The test case conditions are such that the electrons are in equilibrium with the heavy particles, or the coupling between heavy-particle translational and vibrational temperature was so weak that the present model, which assumed the weak coupling between vibrational and electron temperature, could not properly describe the high-temperature air. With shock slip, the ionization and relaxation behind the shock may produce some difference between the two temperatures, and the modifications necessary for including shock slip into the code are being studied.

Figure 3 shows the electron number density in the shock layer at $s/Rn = 8.8$ for case 1 at $\alpha = 0$ deg for the freestream velocity 7620 m/s. The difference in electron number density predicted by the two models is very small, and this is expected from the small differences in the temperature levels observed. Shock-slip conditions were introduced into the one-temperature code, and the electron number density with shock slip is about two orders of magnitude higher than that for the no-shock-slip case. The results from a seven-species chemical reaction model (O, O_2, N, N_2, NO^+, NO, and e^-) are presented for comparison, and the seven-species model underpredicts the flight data.

Figure 4 shows the electron- and heavy-particle temperature profiles at $s/Rn = 8.8$ for case 1 at $\alpha = 5$ deg for both windward and leeward planes, where the electron temperature is almost identical to the heavy-particle temperature. Figure 5 shows the electron number density profiles at $s/Rn = 8.8$ for case 1 at $\alpha = 5$ deg. Again both one- and two-temperature models predict nearly the same electron number density.

Figures 6-8 show the effects of the two-temperature model on the surface-measurable quantities for case 1 at $\alpha = 0$ deg. The calculation was performed assuming no shock slip and a fully catalytic wall. The surface pressure normalized by the freestream pressure is plotted against the streamwise coordinate normalized by the nose radius in Fig. 6. The pressure distribution is essentially the same from both the one- and two-temperature models. Figures 7 and 8 show the surface heat-transfer and streamwise skin-friction distributions, re-

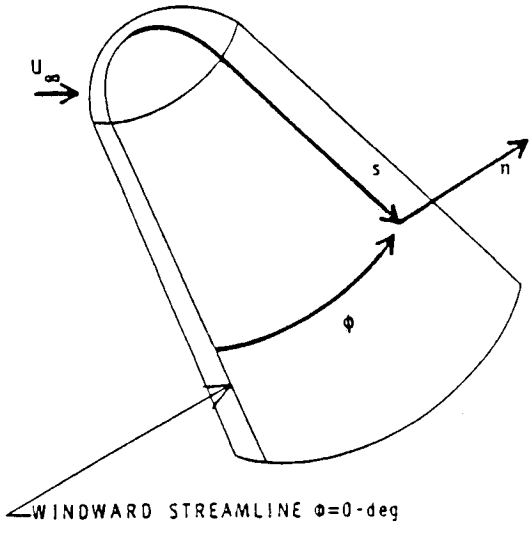

Fig. 1 Coordinate system.

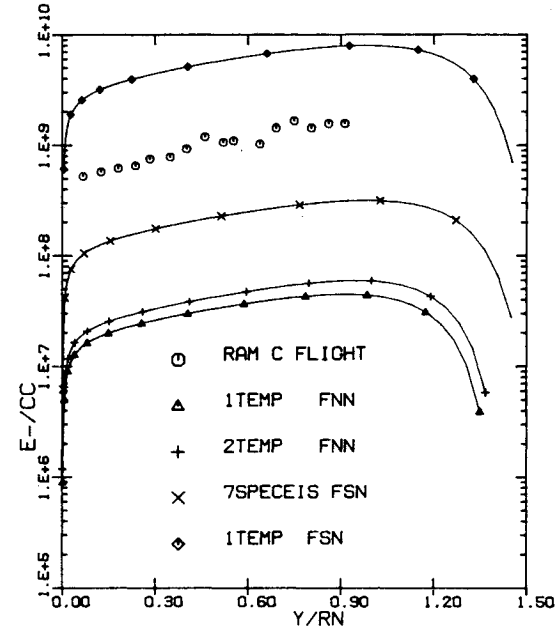

Fig. 3 Electron density profile at $s/Rn = 8.8$ for case 1 at $\alpha = 0$ deg.

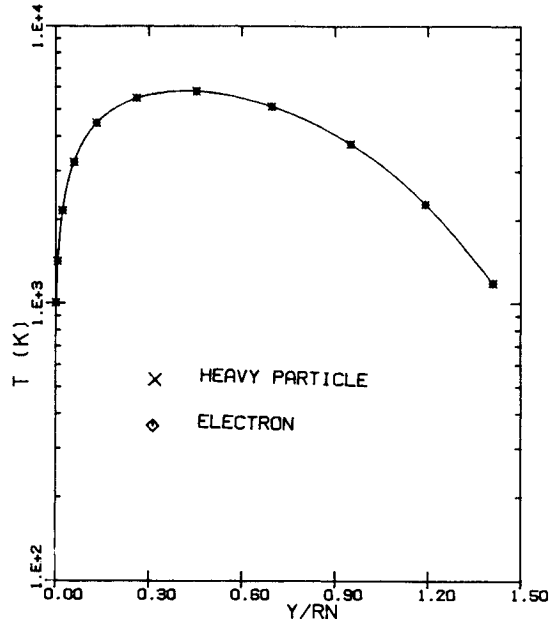

Fig. 2 Temperature profile at $s/Rn = 8.8$ for case 1 at $\alpha = 0$ deg.

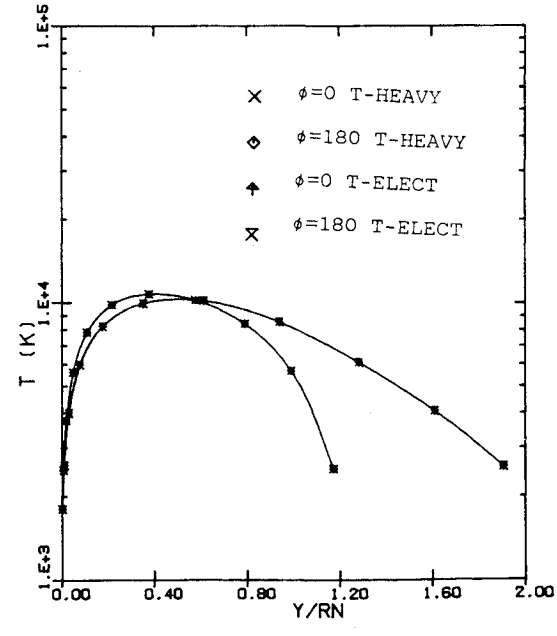

Fig. 4 Temperature profile at $s/Rn = 8.8$ for case 1 at $\alpha = 5$ deg.

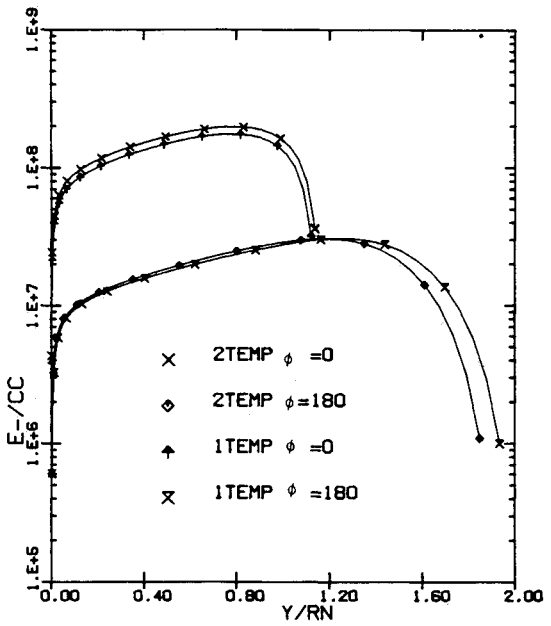

Fig. 5 Electron density profile at $s/Rn = 8.8$ for case 1 at $\alpha = 5$ deg.

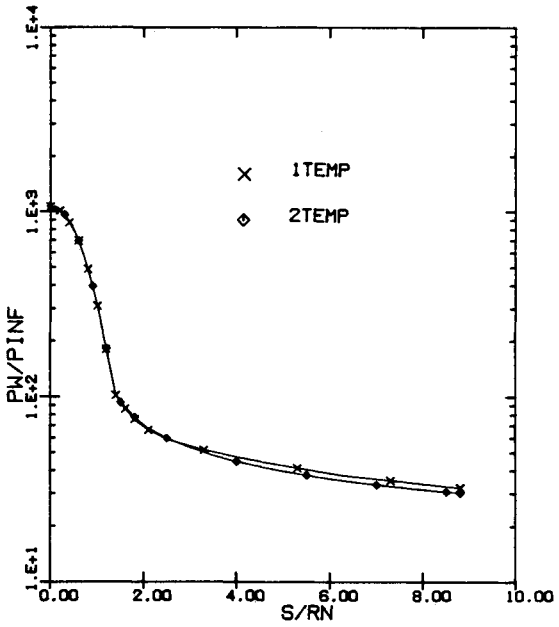

Fig. 6 Effect of two-temperature model on surface pressure distribution for case 1 at $\alpha = 0$ deg.

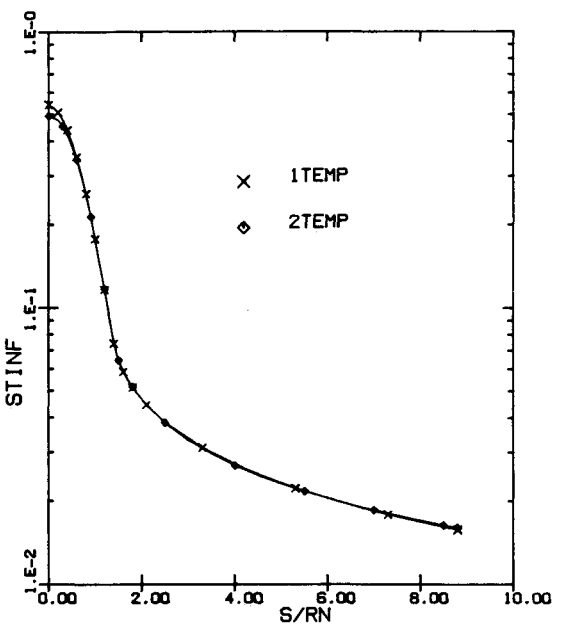

Fig. 7 Effects of two-temperature model on surface heat-transfer distribution for case 1 at $\alpha = 0$ deg.

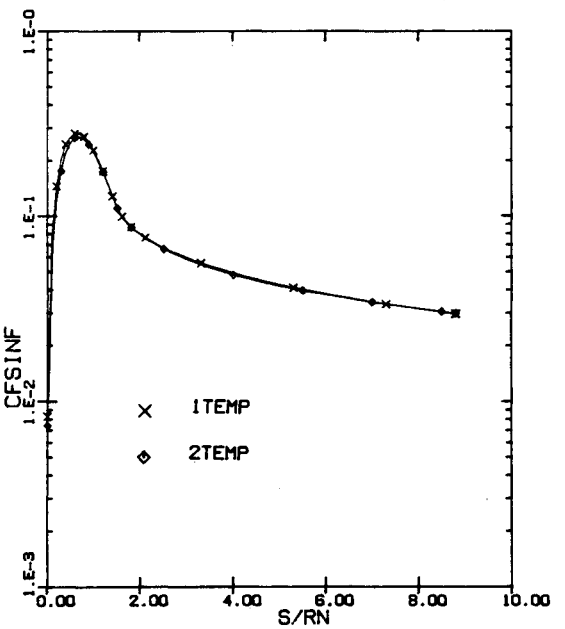

Fig. 8 Effects of two-temperature model on streamwise skin-friction distribution for case 1 at $\alpha = 0$ deg.

spectively, for the same case. The two-temperature model predicts essentially the same result as the one-temperature model over the length of the body. The effects of the two-temperature model on the surface-measurable quantities are smaller than those on the temperature and electron density profiles.

Figures 9 and 10 show the results for case 2 at $\alpha = 0$ deg. Here again the no-shock-slip conditions and a fully catalytic wall were assumed. The electron-temperature profile at $s/Rn = 8.8$ is compared to the heavy-particle temperature in Fig. 9. The agreement between the two temperature profiles is very good. For the velocity of 10,606 m/s (35,000 ft/s) the maximum difference between the electron and heavy-particle temperature is about 61 K. Figure 10 shows the electron number density predicted by both one- and two-temperature models. The electron number density predicted by the two-temperature model is slightly lower than that predicted by the one-temperature model. The results for case 2 show that the two-temperature model without shock slip has little affect on the profiles. This is due to the approximation involved in the no-shock-slip case, where the shock is assumed to be frozen to chemical reactions across the shock wave.

Table 2 shows the computing time for the two test cases considered. The two-temperature model consistently required more time than the one-temperature model by a factor of 1.5. The computing time is based on IBM 370/3081 H = OPT2 complier.

Table 2 Computing times[a]

Geometry[b]	α, deg	U_∞, m/s	Method	ξ From	ξ To	Grid size ξ steps	Grid size η points	Grid size ζ planes	Time m:s	Time ratio[c]
RAM C	0	7620	1-temp	0.0	8.8	35	51	1	2:55	1.00
	0	7620	2-temp	0.0	8.8	35	51	1	4:28	1.53
	0	10606	1-temp	0.0	8.8	35	51	1	3:51	1.00
	0	10606	2-temp	0.0	8.8	35	51	1	5:08	1.33
	5	7620	1-temp	0.0	8.8	35	51	9	24:54	1.00
	5	7620	2-temp	0.0	8.8	35	51	9	38:41	1.55

[a]CPU time on IBM 370/3081, H = OPT2 compiler. [b]RAM C = 9-deg sphere cone. [c]Nonequilibrium 11-species one-temperature model is taken as reference.

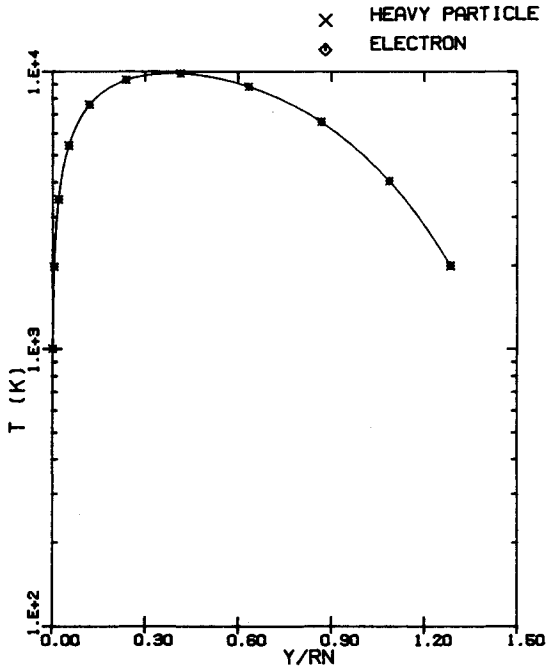

Fig. 9 Temperature profile at $s/Rn = 8.8$ for case 2 at $\alpha = 0$ deg.

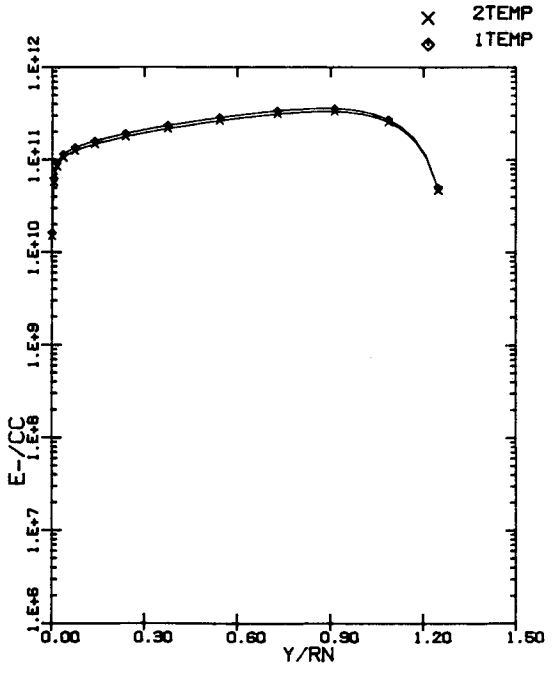

Fig. 10 Electron density profile at $s/Rn = 8.8$ for case 2 at $\alpha = 0$ deg.

Concluding Remarks

A numerical method for analyzing three-dimensional nonequilibrium flows over straight and bent multiconics using a two-temperature model has been developed. For the test cases considered, the two-temperature model without shock slip predicted negligible effects on the wall-measurable quantities. For the re-entry problem, the two-temperature model showed no significant change in the electron number density. The maximum difference between the electron temperature and heavy-particle temperature was less than 200 K. In general, the two-temperature model without shock slip had little effect on the electron number density and temperature.

In conclusion, a numerical method for analyzing the three-dimensional nonequilibrium hypersonic viscous shock-layer flows over sphere cones at moderate angles of attacks using both one- and two-temperature models has been developed which predicts the complete flowfield in a reasonable computing time.

Appendix A

Electron Energy Equation for High-Temperature Air

The electron temperature can be obtained from the solution of the electron energy equation. The change in electron energy is the sum of energy exchanged by elastic and inelastic collisions between the electron and heavy particles, where inelastic collision are those that result in ionization of the heavy particles with resulting losses in electron energy. A discussion of the electron energy equation for a nonequilibrium gas is given by Appleton and Bray.[19] The electron energy equation for a hydrogen-helium system has been given by Leibowitz,[4] and in this paper the same procedure is applied to high-temperature air.

Consider the direct ionization of oxygen and nitrogen by electron-atom collision

$$O + e^- = O^+ + e^- + e^-$$

$$N + e^- = N^+ + e^- + e^-$$

For a one-dimensional steady shock wave, the resulting electron energy equation for nonequilibrium air is

$$\frac{\partial}{\partial y}(\epsilon_e u) = 3[e] m_e \bar{\nu} R (T - T_e) - \theta_O (R_1 - R_{1r}) - \theta_N (R_2 - R_{2r})$$

where

ϵ_e = energy per unit volume of the electron, $\epsilon_e = 3/2\ [e] R T_e$
y = distance behind shock wave
$[e]$ = concentration of electron
m_k = mass of species k
Q_{ek} = elastic collision cross section for species k
ν_{ek} = collision frequency for elastic collision between electron and species k, $\nu_{ek} = n_k v_e Q_{ek}$

n_k = molar concentration of species k
v_e = average electron velocity, $(8kT_e/\pi m_e)^{1/2}$
θ_k = ionization energy per mole of species k
$\bar{\nu}$ = $\Sigma \nu_{ek}/m_k$
R_i, R_{ir} = the forward and reverse reaction rates for electron production

A steady-state condition corresponds to the case where the energy is used by the electron for ionization at the same rate as it is received from elastic collision. In this case, setting the right-hand side to zero,

$$3[e]m_e\bar{\nu}R(T-T_e)-\theta_O(R_1-R_{1r})-\theta_N(R_2-R_{2r})=0$$

By solving for T_e,

$$T_e = T-(X_2k_{f1}-X_3k_{b1}+X_4k_{f2}-X_5k_{b2})/X_1$$

where

$$X_1=3m_e\bar{\nu}R, \quad X_2=\theta_O[O], \quad X_3=\theta_O[O^+][e],$$

$$X_4=\theta_N[N], \quad \text{and} \quad X_5=\theta_N[N^+][e]$$

The fluid dynamic variables, species concentration, and electron temperature are found by simultaneously solving the fluid mechanics equations, species conservation equations, and electron energy equations.

References

[1]Swaminathan, S., Song, D. J., and Lewis, C. H., "Effects of Slip and Chemical Modeling on Three-Dimensional Nonequilibrium Viscous Shock-Layer Flows," *Journal of Spacecraft and Rockets,* Vol. 21, Nov.-Dec. 1984, pp. 521-527.

[2]Park, C., "Problems of Rate Chemistry in the Flight Regimes of Aeroassisted Orbital Transfer Vehicles," AIAA Paper 84-1730, Jan. 1984.

[3]Leibowitz, L. P. and Kuo, Ta-Jin, "Ionizational Nonequilibrium Heating During Outer Planetary Entries," *AIAA Journal,* Vol. 14, Sept. 1976, pp. 1324-1329.

[4]Leibowitz, L. P., "Measurements of the Structure of an Ionizing Shock Wave in a Hydrogen-Helium Mixture," *Physics of Fluids,* Vol. 16, Jan. 1973, pp. 59-68.

[5]Tiwari, S. N and Szema, K. Y., "Effects of Precursor Heating on Radiating and Chemically Reacting Viscous Flow around a Jovian Entry body," NASA CR-3186, Sept. 1979.

[6]Bird, R. B., Stewart, W. E., and Lightfoot, E. N., *Transport Phenomena,* John Wiley and Sons Inc., New York, 1960.

[7]Swaminathan, S., "Three-Dimensional Nonequilibrium Viscous Shock-Layer Flows over Complex Reentry Vehicles," Ph.D. Thesis, Virginia Polytechnic Institute and State University, Blacksburg, VA, May 1983.

[8]Swaminathan, S., Kim, M. D., and Lewis, C. H., "Nonequilibrium Viscous Shock-Layer Flows over Blunt Sphere-Cones at Angle-of-Attack," *Journal of Spacecraft and Rockets,* Vol. 20, July-Aug. 1983, pp. 331-338.

[9]Kim, M. D., "Three-Dimensional Nonequilibrium Viscous Shock-Layer Flow over the Space Shuttle Orbiter," Ph.D. Thesis, Virginia Polytechnic Institute and State University, Blacksburg, VA, April 1983.

[10]Solomon, J. M., Ciment, M., Ferguson, R. E., Bell, J. B., and Wardlaw Jr., A. B., "A Program for Computing Steady Inviscid Three-Dimensional Supersonic Flow on Reentry Vehicles, Vol. I, Analysis and Programming," Naval Surface Weapon Center, White Oak, MD, Rept No. NSWC/WOL/TR 77-28, Feb. 1977.

[11]Solomon, J. M., Ciment, M., Ferguson, R. E., Bell, J. B., and Wardlaw Jr., A. B., "A Program for Computing Steady Inviscid Three-Dimensional Supersonic Flow on Reentry Vehicles, Vol. II, User's Manual," Naval Surface Weapons Center, White Oak, MD, Rept. No. NSWC/WOL/TR 77-28, Feb. 1977.

[12]Browne, W. G., "Thermodynamic Properties of Some Atoms and Atomic Ions," General Electric Co., Philadelphia, PA, MSD Engineering Physics TM2, 1962.

[13]Browne, W. G., "Thermodynamic Properties of Some Diatomic and Linear Polyatomic Molecules," General Electric Co., Philadelphia, PA, MSD Engineering Physics TM3, 1962.

[14]Browne, W. G., "Thermodynamic Properties of Some Diatoms and Diatomic Ions at High Temperature," General Electric Co., Philadelphia, PA, MSD Advanced Aerospace Physics TM8, May 1962.

[15]Biolsi, L., Private communications, July 1983.

[16]Kang, S. W., and Dunn, M. G., "Theoretical and Experimental Studies of Reentry Plasmas," NASA CR-2232, April 1973.

[17]Neynaber, R. H., Lawrence, L.M., Marino, E., Rothe, W., Erhard, W.R., and Trujillo, S. M., "Low-Energy Electron Scattering from Atomic Oxygen," *Physical Review,* Vol. 123, July, 1961, pp. 148-152.

[18]Capatelli, M. and Devote, R. S., "Transport Coefficients of High Temperature Nitrogen," *Physics of Fluids,* Vol. 16, Nov. 1973, pp. 1835-1841.

[19]Appleton, J. P. and Bray, K. N., "The Conservation Equations for a Nonequilibrium Plasma," *Journal of Fluid Mechanics.* Vol. 20, Part 4, Dec. 1964, pp. 659-672.